

Complexity in two-point measurement schemes

Ankit Gill,^{*} Kunal Pal[†], Kuntal Pal,[‡] and Tapobrata Sarkar[§]

Department of Physics, Indian Institute of Technology Kanpur, Kanpur 208016, India



(Received 23 November 2023; accepted 20 February 2024; published 6 March 2024)

We show that the characteristic function of the probability distribution associated with the change of an observable in a two-point measurement protocol with a perturbation can be written as an autocorrelation function between an initial state and a certain unitary evolved state by an effective unitary operator. Using this identification, we probe how the evolved state spreads in the corresponding conjugate space, by defining a notion of the complexity of the spread of this evolved state. For a sudden quench scenario, where the parameters of an initial Hamiltonian (taken as the observable measured in the two-point measurement protocol) are suddenly changed to a new set of values, we first obtain the corresponding Krylov basis vectors and the associated Lanczos coefficients for an initial pure state, and define the associated spread complexity. Interestingly, we find that in such a protocol, the Lanczos coefficients can be related to various cost functions used in the geometric formulation of circuit complexity, for example, the one used to define Fubini-Study complexity. We illustrate the evolution of spread complexity both analytically, by using Lie algebraic techniques, and also by performing numerical computations. This is done for cases when the Hamiltonian before and after the quench are taken as different combinations of chaotic and integrable spin chains. We show that the spread complexity saturates for large values of the parameter only when the prequench Hamiltonian is chaotic. Furthermore, in these examples, we also discuss the importance of the role played by the initial state, which is determined by the time-evolved perturbation operator.

DOI: [10.1103/PhysRevB.109.104303](https://doi.org/10.1103/PhysRevB.109.104303)

I. INTRODUCTION

The dynamics of an isolated quantum system, which is taken out of equilibrium, is a topic of great recent interest. This is partly due to the fact that from the experimental point of view, modern ultracold atoms provide an excellent approximation of an isolated quantum system [1,2]. Among the most important questions raised to explain these path-breaking experiments, one of the most fundamental is the possible mechanism behind the emergence of classical thermodynamics from underlying quantum statistical mechanics.

To this end, recall that one of the most commonly used concepts associated with a classical thermodynamical process is the work done on a system. This is, however, not an observable in one of the canonical ways of defining the work done on quantum systems: the so-called two-point measurement (TPM) scheme [3–6]. The reason is that the definition of work \mathcal{W} associated with a quantum process (as measured through a TPM scheme) involves two projective energy measurements of the system. One of these is carried out at an initial time before the process, and the other after a unitary evolution by a second Hamiltonian for a time at which we want to make a second measurement on the system. As a result, no Hermitian operator can be associated with \mathcal{W} , and hence this is not an observable [6]. Actually, one needs to perform the above measurements on infinitely many realizations of the same system,

and the work is described by a probability distribution $P(\mathcal{W})$. The fluctuation of work in a generic thermal quantum system then comes from both the thermal and quantum mechanical fluctuations.

An important quantity that elucidates many universal features associated with the above notion of work statistics is the Fourier transform of the work probability distribution function, i.e., the characteristic function (CF) of work distribution

$$G(u) = \int P(\mathcal{W}) e^{-iu\mathcal{W}} d\mathcal{W}. \quad (1)$$

Here, the auxiliary variable u is the conjugate of the work done on the system. Importantly, as shown in [6] (see also [7]), the above CF can be interpreted as a correlation function corresponding to the u evolution. For example, in a sudden quench protocol, where one changes the parameters of an initial Hamiltonian suddenly at an instant of time to a new set of values, the CF is just the Loschmidt amplitude, i.e., the overlap between the initial state and a u -evolved state [7]. In a related but somewhat different context, the work of [8] showed how the CF of the work distribution (WD) in the TPM protocol with a perturbation operator inserted instantly, can be written as an out-of-time ordered correlator (OTOC) [9,10] between certain operators. As a result, it was also possible to draw a connection between the dynamics of information scrambling, as quantified by the OTOC, and thermodynamically fluctuating quantities like work in such a protocol.

Another important relation connecting the quantum thermodynamic quantities like WD and the Loschmidt echo (LE) was established in [11], where it was shown that for an isolated quantum system in a generic mixed state, the

^{*}ankitgill20@iitk.ac.in

[†]kunalpal@iitk.ac.in

[‡]kuntal@iitk.ac.in

[§]tapo@iitk.ac.in

CF of work under a quantum quench is related to the LE amplitude in a larger Hilbert space of an auxiliary system, representing the purification of the initial density matrix, and that the quench can be thought of as acting on a single copy of this auxiliary system. In this context, it can be noted that the LE, which measures the overlap of an initial state with a state that has undergone a forward evolution by the system Hamiltonian, and a subsequent backward time evolution by a slightly perturbed Hamiltonian, is a widely used measure in quantum chaos literature [12–15].

This set of results points towards an underlying connection between the fluctuations of thermodynamic quantities associated with the nonequilibrium dynamics of an isolated quantum system and the chaotic or integrable nature of the Hamiltonian governing the unitary dynamics itself. As the CF contains the dynamics of an auxiliary system where the role of time is played by the scalar parameter [denoted in Eq. (1) as u] which, in general, is the Fourier conjugate variable of the eigenvalue of the operator which is measured in the TPM scheme, this also encodes the full information of work PDF. In particular, this connection was firmly established in [11], where it was shown that for certain type of quench protocols with chaotic Hamiltonians, the features of scrambling of information as encoded in the LE, which shows the characteristic dip, ramp, and plateau structure, can also be accessed by the corresponding CF, and hence the associated WD. This is the link we pursue further in this paper by using the tools of quantum complexity theory, particularly the Krylov complexity (KC), a new measure of the “complexity” of a time-evolved operator that has been used extensively in recent times to probe the dynamics quantum chaotic systems and the physics of information scrambling.

The KC, a new addition to the dictionary of the complexity of quantum systems, was originally introduced in the context of measuring operator growth in quantum-many-body systems in [16]. After the original work, the central result of which introduced a hypothesis about the growth of the so-called Lanczos coefficients (LCs), KC has become a very fruitful measure to study various aspects of quantum systems, both in and out of equilibrium. For a partial set of works, see [17,18] for the use of KC in operator growth, [19–21] for works in CFTs, [22–24] for works on open systems, [25] for KC in bosonic systems, [26] as a tool of probing delocalization properties in integrable quantum systems, [27,28] focuses on billiard systems. Important steps have also been taken to understand features of KC in QFTs [29,30]. Various other features and uses of KC were also explored in [31–50].¹

A related but somewhat different concept of the so-called Krylov state complexity or spread complexity (SC) was first introduced in [51], where it was proved that a certain cost associated with the spread of a quantum state under a Hamiltonian evolution with respect to a fixed set of basis vector on the Hilbert space is minimized only if the basis vector is taken as the Krylov basis generated by the Hamiltonian. The

Krylov basis is a set of orthonormal vectors on the Hilbert space that can be constructed using the Lanczos algorithm [52,53], and for a Hamiltonian evolution, this algorithm generally gives two sets of LCs. After the original work of [51], SC in quantum systems has been explored in various papers that include quantum phase transition [54–56], work statistics in quantum quenches [57,58], probing quantum scar states [59], systems described by random matrices [60], studying integrability to chaos transition [61], interacting quantum systems [62], among others.

One of our primary goals is to unify two different kinds of observables, namely, quantum information theoretical [such as the entanglement entropy, OTOC, complexity, etc. (see [63–67])] and quantum thermodynamical [such as the work performed, heat generated, etc. (see [7,68,69])], that are commonly employed to study evolution of a quantum system subjected to quenches. In our previous work [57], we obtained one such relation, where we showed that the LCs associated with the evolution generated by the postquench Hamiltonian can be obtained from the average, variance, and higher-order cumulants of the distribution of the work done on a system through a sudden quench, thereby providing interpretations of these coefficients in terms of experimentally observable quantities.

In this work, we proceed with a similar motivation, and first discuss a connection between the two concepts mentioned in the previous paragraphs, namely, CF associated with probability distribution of an observable in a TPM scheme and the complexity of the spread of a certain unitary evolved state, by noting that the CF of a TPM scheme (with a perturbation operator W introduced between a forward and backward evolution) can be equivalently viewed as an autocorrelation function (ACF) corresponding to the evolution generated by the Hermitian operator (denoted as O in subsequent analysis) which is measured under a TPM scheme (see Sec. II B). This naturally leads us to define a set of Krylov bases generated by the observable O , and the concept of SC associated with the u -evolved state in Sec. III. This will help us to probe the unitary evolution in the space that is Fourier conjugate to the observable O , the change of which is measured in a TPM protocol, by using the tools of Krylov state complexity. The fact that the full set of LCs, and consequently the full Krylov basis sets, can be extracted from the knowledge of the ACF, we are able to study the behavior of SC both analytically and numerically in Secs. IV and V, respectively. In particular, we will show how the integrable or chaotic nature of the operator O (which can be taken as the Hamiltonian of some quantum system H) differentiates the spreading of information in the conjugate u space.

In a similar spirit, we establish relations between the fidelity OTOC (FOTOC), the survival probability of the u -evolved state, and the corresponding LCs, and show that in the sudden quench protocol, when O is the Hamiltonian H_0 , the LC b_1 is the Fisher information of the time-evolved state. Furthermore, in Sec. VI, we show that the nature of the inverse participation ratio (IPR) of the time-evolved state is directly related to the nature of the LCs of the u -evolved state, and verify this connection using an analytical example with the Hamiltonian taken as an element of the $\mathfrak{su}(1, 1)$ Lie algebra. Finally, in Sec. VII, we discuss possible importance of our

¹There are a large number of works on various aspects of KC and operator growth, so the list of references mentioned above is incomplete. For a more complete account of various avenues explored the reader can look at the citations of the papers mentioned here.

results from the point of view of experiments that are used to measure the WD, and the subsequent possibility of relating SC with experimentally measurable quantities.

II. OUT-OF-TIME ORDER CORRELATORS FROM TWO-POINT MEASUREMENT PROTOCOLS

The OTOC was first introduced in [9] to study the instability of electron trajectories in superconductors. For two generic Hermitian (or unitary operators) V and W , it is defined as

$$C_{V,W}(t) = \langle [W_t, V]^\dagger [W_t, V] \rangle, \quad (2)$$

where $W_t = e^{-iHt} W e^{iHt}$ represents time-evolved form of the initial operator $W = W(t=0)$ under the Hamiltonian H . After the work of [10], this quantity has been used extensively to study quantum chaos. Expanding the expression for the correlator $C_{V,W}(t)$, we see that it contains terms where the operators are ordered in out-of-time fashion (in contrast to the usual time-ordered correlators). Among such terms, in this paper, our interest will be a term of the form

$$F_{V,W}(t) = \langle W_t^\dagger V^\dagger W_t V \rangle, \quad (3)$$

which, as we shall see, can be recasted as an ACF. Since $\text{Re}[F_{V,W}(t)] = 1 - \langle [V^\dagger, W_t^\dagger][W_t, V] \rangle / 2$, we see that this quantity actually measures the amount by which the operators W_t and V fail to commute at a later time t under the evolution by the Hamiltonian H , provided that the operators W and V commute at the initial time $t = 0$.

In quantum systems, the OTOC can be used as one of the diagnostic tools of quantum chaos at the level of dynamics. For systems that have a well-defined semiclassical limit, or systems that have a large number of local degrees of freedom, one can characterize quantum chaos from the short-time exponential growth of OTOC [10]. Physically, OTOC measures how quantum information, which was initially in some local subsystem, becomes delocalized in the entire system. This “spread” of local information to the entire system is usually called the scrambling of quantum information. One can quantify this spreading by using the growth of a local operator under a Hamiltonian evolution. Mathematically, one way to do this is to use the squared commutator in Eq. (2), where, as we have mentioned above, two initially commuting operators will no longer commute due to the fact that the operator W gets “complicated” due to the time evolution.

Another way one can measure how an operator or a quantum state gets complicated under a Hamiltonian evolution is by counting the support of a time-evolved state or an operator in terms of a specified orthonormal basis, known as the Krylov basis. The resulting measure, the KC or the SC discussed in the Introduction, has gained wide attention recently due to the fact that it is another very useful tool for characterizing quantum chaos since the corresponding sets of LCs as well as this measure of complexity show particular behavior for quantum chaotic systems [16,51]. In this paper, we define a special class of SC from the OTOC, which quantifies how the initial state of a quantum system that has been perturbed far from equilibrium through a sudden quench spreads under evolution generated by the initial Hamiltonian.

A. Two-point measurement schemes

We start by briefly describing the protocol considered in this paper. Due to the appearance of out-of-time order operators discussed above, it is difficult to measure correlators experimentally. Recently, using the well-known TPM scheme [3,4], in [8], the authors have proposed an alternative method of measuring these for a wide class of states. In such a TPM scheme, an observable O is projectively measured before and after a nonequilibrium process (such as a quantum quench) is performed on a quantum system.

In [8], one such protocol was considered, and it contains the following steps: (1) A quantum system (with a Hamiltonian denoted by H_0) is prepared in some state ρ at $t = 0$. (2) First projective measurement of an observable O is performed, after which the system collapses to an eigenstate $|O_n\rangle$ of the observable, and giving a result O_n , the n th eigenvalue of the operator O . (3) For $t > 0$ the system is evolved with a Hamiltonian H for a time $t = \tau$. (4) After this time, a unitary perturbation W (known as the wing-flap operator) is applied to the system. (5) The system is evolved with $-H$ for a time $t = \tau$, and finally, (6) a second projective measurement of O is performed which now yields a value O_m , thereby collapsing the system to the eigenstate $|O_m\rangle$ of O . For a schematic representation of this protocol, see Fig. 1 of Ref. [8].

Due to the presence of the perturbation W , the state of the system after the evolution with $-H$ [the backward evolution, step (5) of the above protocol] is not the same as the initial state $|n\rangle$; rather, it can be thought of as a linear combination of all the eigenstates of O . Therefore, the second projective measurement can select any one of these states, and hence $|O_m\rangle$ can be different from the initial state.

Since after the second measurement the eigenvalue can take any of the possible values O_m , by repeating the above protocol a very large number of times, we can obtain a probability distribution function (PDF) for the change in the value of the operator O due to the perturbation W . The PDF for the change of the observable $\Delta O = O_m - O_n$ is given by the expression

$$P(\Delta O, \tau) = \sum_{n,m} P_\tau[O_m|O_n] p_n \delta(\Delta O - (O_m - O_n)), \quad (4)$$

where p_n denotes the probability of getting an outcome O_n after the first measurement of the observable O , and $P_\tau[m|n]$ gives the probability of obtaining the result O_m after the second measurement with the condition that the first measurement yields a value O_n . For the TPM protocol described above, the expression for this quantity can be written as

$$\begin{aligned} P_\tau[O_m|O_n] &= |\langle O_m | e^{i\tau H} W e^{-i\tau H} | O_n \rangle|^2 \\ &= |\langle O_m | W_\tau | O_n \rangle|^2, \end{aligned} \quad (5)$$

where W_τ denotes the operator W at time τ in the Heisenberg representation, i.e., $W_\tau = e^{-iH\tau} W e^{iH\tau}$. Here we assume that the observable O has nondegenerate spectrum and that the condition $[\rho, O] = 0$ is satisfied.

Next we need to consider the CF of the above PDF in Eq. (4), which is defined as the Fourier transform of $P(\Delta O, \tau)$:

$$G(u, \tau) = \int P(\Delta O, \tau) e^{-iu\Delta O} d(\Delta O). \quad (6)$$

The auxiliary variable u , which appears as the conjugate of ΔO , is sometimes called the second time of evolution in the literature [7,11].

The significance of this quantity for our purposes can be understood as follows. Suppose we perform a sudden change in the parameters of a quantum system, i.e., the system is subjected to a quench, so that the Hamiltonian of the system is changed from H_0 at $t = 0$ to H and the system is subsequently evolved with the new Hamiltonian. If we measure the energy of the system before and after such a change, i.e., the operator O is the Hamiltonian of the system, then the change in the energy $\mathcal{W} = E_n^0 - E_m$ of the system is the work done on the system due to this quench. Assuming that the system was prepared in an eigenstate $|0\rangle$ of the prequench Hamiltonian, the CF of the WD can be recasted as a correlation function of the form [6]

$$G(t) = \langle 0 | e^{iH_0 t} e^{-iH t} | 0 \rangle = e^{iE_0 t} \langle \psi_0 | \Psi(t) \rangle, \quad (7)$$

where $|\Psi(t)\rangle$ denotes the time-evolved state after the quench, and t denotes the time after the quench, and here it is conjugate to the work done \mathcal{W} . As was established in [7], this is just the Loschmidt amplitude,² a quantity used extensively to study quantum quenches and quantum chaos [12–15]. Although here we have shown it for initial pure states, however, this identification is still valid for arbitrary initial mixed states as well. Furthermore, as we have shown previously in [57] the fact that the CF of the WD is just the ACF implies that this contains the information about the LC corresponding to the evolution generated by the postquench Hamiltonian, and, therefore, also determines the spread of the time-evolved wave function in the Hilbert space. Here, our goal is to establish a similar relationship between the CF and the ACF for the TPM scheme in the presence of the perturbation W .

B. OTOC in a two-point measurement scheme as an autocorrelation function

We now find out the CF for the TPM scheme described at the beginning of Sec. II A. Substituting the distribution in Eq. (4) into the definition of the CF in Eq. (6) and using the resolution of the identity satisfied by the eigenstates of the operator O we arrive at the relation [8]

$$G(u, \tau) = \langle O_0 | W_\tau^\dagger V^\dagger W_\tau V | O_0 \rangle = F_{V,W}(\tau),$$

$$\text{where } V = e^{iuO}. \quad (8)$$

This computation, therefore, shows that the CF of the distribution of ΔO in a TPM scheme is just the OTOC between the perturbation operator W and $V = e^{iuO}$, where O is the operator whose change is measured during the protocol. Since the OTOC is used to probe the scrambling of quantum information, the above identification indicates that CF of the distribution of ΔO , and hence the probability distribution itself (which is related to the CF through a Fourier transform), encodes the nature of information scrambling in a quantum system after it is subjected to a nonequilibrium protocol such

as a quantum quench. Therefore, this helps to understand the scrambling of information from a thermodynamic perspective (this will be discussed in Sec. III C below as well). For more details about the relation between the information scrambling, LE, and statistics of work done in chaotic quantum systems see [11,70].

We now show that by suitably rewriting the relation in Eq. (8), it can also be argued that the OTOC $F_{V,W}(\tau)$ also contains information about the LC of the evolution generated by the operator O itself, i.e., it determines the spread of a certain initial state in the Hilbert space corresponding to the operator O . To show this, we proceed as follows. First, from Eq. (8) it can be seen that we can write the CF as

$$\begin{aligned} G(u, \tau) &= e^{iuO_0} \langle O_0, \tau | e^{-iuO} | O_0, \tau \rangle \\ &= e^{iuO_0} \langle O_0, \tau | O_0, \tau, u \rangle, \end{aligned} \quad (9)$$

where we have defined $|O_0, \tau\rangle = W_\tau |O_0\rangle$. If W is a unitary operator, this is just the state at time τ evolved by the time-dependent operator W_τ . Now we see that (apart from an overall phase factor) the function $G(u, \tau)$ can be thought of as the (conjugate of) the ACF between the evolved state $|O_0, \tau, u\rangle = e^{-iuO} |O_0, \tau\rangle$, and an initial state $|O_0, \tau\rangle$. The state $|O_0, \tau, u\rangle$ is therefore an evolved state in the second time of evolution u . Also, as far as the evolution through u is concerned, the initial state $|O_0, \tau\rangle$ is time independent. In this picture, we can think of the ACF corresponding to that of a sudden quench performed on an auxiliary system described by an auxiliary Hamiltonian O , such that the initial parameters of an operator O_0 are suddenly changed to a new set of values at $u = 0$, and the subsequent evolution in u is generated by the new auxiliary Hamiltonian O .

The discussion above indicates that the ACF, which is just the OTOC between W_τ and V , as well as the CF corresponding to the distribution of the change of an observable O in a TPM protocol, also has the information of the spreading of the initial state $|O_0, \tau\rangle$ in the Krylov subspace generated by the operator O . As the next step, we define the SC corresponding to the u evolution, and find out the associated Krylov basis and LCs. This is what we describe in the next section.

However, before moving on to the next section, here we note the following points. First, from now on, we shall neglect the overall constant phase factor in front of the ACF in Eq. (9). The effect of this phase factor is just to shift the average values of ΔO , and does not have any extra physical meaning [57]. In fact, this phase factor can be set to unity by adjusting the lowest eigenvalue of O to zero (i.e., $O_0 = 0$).

Second, as we elaborate upon below, the basic idea behind the notion of the SC is to write a time-evolved³ evolved state (generated by some Hermitian operator, such as the

²This is also the ACF between the time-evolved state and the initial state before the quench.

³Here, the time can be the time parameter appearing in the time-dependent Schrödinger equation, or it can be an auxiliary parameter conjugate to the eigenvalue of some observable (such as the parameter u above). In the second case, we also call them the circuit time, in analogy with the nomenclature used in the definition of the Nielsen and related related geometric measures of circuit complexity, where the evolution is generated in the circuit space by some suitable unitary operator.

Hamiltonian of a quantum system) in terms of an orthogonal and complete basis, and find out the projection of the time-evolved state in terms of the elements of the basis. These projections, usually denoted as $\phi_n(u)$, are just the probability amplitudes of obtaining the evolved state in each of these basis vectors. The SC is defined as the minimum (obtained in a special basis known as the Krylov basis) of the weighted sum of the modulus squared of ϕ_n , and measures the spread of the evolved state in that basis. When the first state of the basis is the initial state at the start of the evolution ($u = 0$), $\phi_0(u)$ is just the ACF. Therefore, for the evolution denoted in Eq. (9), we see that the OTOC is $\phi_0(u)$. For the case where the Krylov basis has only two elements, the OTOC completely determines the spreading of the initial state. However, in the more general case with higher number of Krylov basis elements, the OTOC between W and V does not have information about ϕ_n 's with $n \geq 1$. In those cases, the SC of the u evolution defined in the next section is more useful for studying the propagation of the initial state with circuit time, and, in a sense, has more information than standard OTOC.

Finally, we note that, in this paper we assume that the initial state of the system is a pure state (which we denote as $|O_0\rangle$), so that the CF associated with the distribution of Eq. (4) can be directly interpreted as an ACF. However, this conclusion can not be straightforwardly extended to the cases where the initial state is a mixed state with density matrix ρ_0 . To understand this, we notice that for initial mixed states of the form $\rho_0 = \sum_n p_n^0 |O_n\rangle\langle O_n|$, the CF can be written as

$$\begin{aligned} G(u, \tau) &= \sum_n p_n^0 \langle O_n | W_\tau^\dagger e^{-iuO} W_\tau e^{iuO} | O_n \rangle \\ &= \sum_n p_n^0 e^{iuO} \langle O_n, \tau | e^{-iuO} | O_n, \tau \rangle. \end{aligned} \quad (10)$$

Now it can be seen that $G(u, \tau)$ can not be directly written as an ACF (or Loschmidt amplitude). One way to proceed for such initial mixed states is to purify the initial density matrix by embedding it in a double-copy Hilbert space, so that, as in [11], the CF can be written as an ACF with respect to the double-copy states. The resulting definition of SC in such cases is beyond the scope of this paper, and we hope to return to this issue in a future work.

III. SPREAD COMPLEXITY OF u EVOLUTION IN A TWO-POINT MEASUREMENT PROTOCOL

A. Definition of the spread complexity of u evolution

Using the identification between the OTOC in the real-time evolution and the ACF corresponding to the u evolution obtained in the previous section, here we extend the definition of SC such that it captures the properties of the u evolution of an initial state in a TPM scheme.

We first describe the Lanczos algorithm for constructing the Krylov basis and the subsequent definition of the SC of an initial state $|O_0, \tau\rangle$ under evolution generated by the operator O . The Krylov basis is used to write the operator O in a tridiagonal form. In this construction, we start from the initial

state $|\tilde{K}_0\rangle = |O_0, \tau\rangle$,⁴ i.e., we take the first state of the Krylov basis as the initial state at $u = 0$, and a new element of the basis is obtained from the old ones as follows:

$$|\tilde{K}_{n+1}\rangle = \frac{1}{\tilde{b}_{n+1}} [(O - \tilde{a}_n)|\tilde{K}_n\rangle - \tilde{b}_n|\tilde{K}_{n-1}\rangle]. \quad (11)$$

The sets of coefficients \tilde{a}_n and \tilde{b}_n are the LCs,⁵ and these can be obtained from the moments of the ACF given in Eq. (9) (see Ref. [52] for details of this procedure). The first set of coefficients \tilde{a}_n 's are given by the expectation values of the operator O in each of the Krylov basis elements

$$\tilde{a}_n = \langle \tilde{K}_n | O | \tilde{K}_n \rangle, \quad (12)$$

and the second set of coefficients \tilde{b}_n are used to fix the normalization of each $|\tilde{K}_n\rangle$ to unity. We have to stop the recursion when $\tilde{b}_n = 0$ at any particular step. After obtaining the Krylov basis, we can expand the evolved state in terms of this basis

$$|O_0, \tau, u\rangle = \sum_n \tilde{\phi}_n(\tau, u) |\tilde{K}_n\rangle, \quad (13)$$

where the summation is over the dimension of the Krylov basis. Substituting this expansion in the Schrödinger-type equation satisfied by $|O_0, \tau, u\rangle$, we obtain the following discrete equation satisfied by $\tilde{\phi}_n(u)$:

$$i\partial_u \tilde{\phi}_n(u) = \tilde{a}_n \tilde{\phi}_n(\tau, u) + \tilde{b}_n \tilde{\phi}_{n-1}(\tau, u) + \tilde{b}_{n+1} \tilde{\phi}_{n+1}(\tau, u). \quad (14)$$

To arrive at the associated notion of the SC, we first define the cost function $\mathcal{C}_B(u) = \sum_n n |\langle O_0, \tau, u | B_n \rangle|^2$, which can be thought of as a measure of the spreading of the time-evolved state in an arbitrary complete orthonormal basis $|B_n\rangle$. It was recently shown that [51] for an evolution generated by a time-independent Hermitian operator, the basis which minimizes this particular cost function is the Krylov basis constructed using that Hermitian operator. For our case, this operator is the observable O , and using the expansion in Eq. (13) we arrive at the following definition of the SC in this case:

$$\mathcal{C}(\tau, u) = \sum_n n |\langle O_0, \tau, u | \tilde{K}_n \rangle|^2 = \sum_n n |\tilde{\phi}_n(\tau, u)|^2. \quad (15)$$

The reason we have also included the τ parameter in the definition of the SC will be explained below shortly.

B. Implications of the complexity of u evolution

With this definition of the SC of circuit time evolution, we now explore some of its consequences. First, notice that, though this definition of the SC is similar to the SC of usual Hamiltonian evolution, here it also has information of the time evolution of the W operator through the initial state $|O_0, \tau\rangle$. The more “complicated” the W operator becomes with evolution through the system Hamiltonian H , the initial state of the circuit evolution gets more complicated. Thus,

⁴Here, we have used an overall tilde in the notation for the Krylov basis elements to distinguish these from the Krylov basis generated through the Hamiltonian evolution.

⁵Once again, we have used an overall tilde to distinguish these from the LC generated in the Hamiltonian evolution.

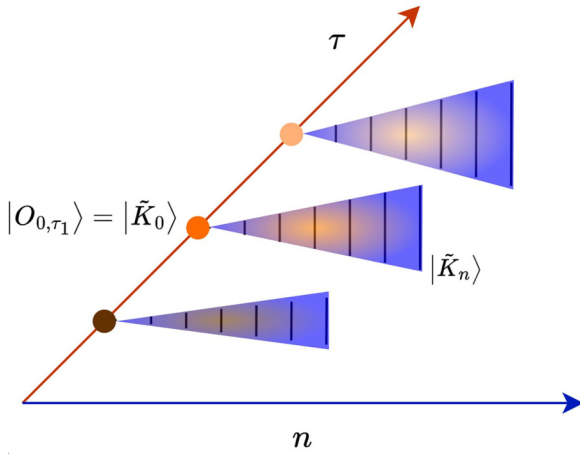


FIG. 1. A schematic illustration of the spreading associated with the parameter u for different initial states, corresponding to the different values of τ , the time where the perturbation operator is applied. The horizontal axis is marked as n to indicate the spreading of the u -evolved state in the Krylov basis $|\tilde{K}_n\rangle$ generated by the operator O .

both the system Hamiltonian for $t > 0$, as well as the wing-flap perturbation operator W , influence the behavior of the SC $\mathcal{C}(\tau, u)$ through the initial state $|O_{0, \tau}\rangle$. Therefore, if we consider circuit evolution by the same operator O of two initial states corresponding to the parameters, say τ_1 and τ_2 , depending upon their relative values the spreading of these two initial states can be very different. This is the reason we have kept the parameter τ in the definition of SC in Eq. (15), even though $\mathcal{C}(\tau, u)$ essentially measures the complexity of spreading of an initial state with respect to the circuit time u . In Fig. 1 we provide an illustration of the spreading of the u -evolved state in the Krylov basis generated by the operator O . The axis leveled with τ indicates different initial points of this evolution.

In the following, we therefore consider the SC, $\mathcal{C}(\tau_i, u)$, for initial states with different values of the parameter τ_i , which is the value of time where the perturbation W has been applied on the system. Furthermore, at this point, it is also useful to discuss the role played by the KC of the operator W , and the nature of the Hamiltonian H on the initial state. The KC is the analog of the SC for the evolution of an operator in the Heisenberg picture and was introduced in [16]. The procedure used to define it is very similar to the one used in Eq. (15), i.e., one finds out the Krylov basis $|\tilde{K}_n\rangle$ generated by the Liouvillian superoperator associated with the Hamiltonian generating the operator evolution in the Heisenberg picture (here W_τ is such an operator), and expand the time-evolved operator (written as a state in the Hilbert space of the operator) in the Krylov basis [analogous to Eq. (13)]. The weighted sum of the modulus squared of these expansion coefficients $\phi_n(t)$ defines the KC of the Heisenberg picture operator. Roughly, the more the operator spread in the Krylov basis under Hamiltonian evolution, the higher its Krylov complexity.

Here, in the u evolution, the initial state on which the observable O acts depends on one such time-evolved operator, namely, the perturbation W_τ . Therefore, in some sense, it can be understood that the KC of the operator W_τ should affect the SC of the initial state $|O_{0, \tau}\rangle$.

C. Implications of the Lanczos coefficients and connection with thermodynamics

To understand the significance of the LCs corresponding to the circuit time evolution, in this section we assume that the observable under consideration O is the Hamiltonian H_0 of the system. In this case, the initial state of the system before the u evolution can be denoted as $|E_{00}, \tau\rangle$, where E_{00} is the lowest eigenvalue of the Hamiltonian H_0 , and $G(u, \tau)$ represents the CF corresponding to the probability distribution of the change of the energy $\Delta E_0 (= E_{0m} - E_{00})$ of the initial system due to the perturbation W . Calculating the moments (\tilde{M}_n) of $G(u, \tau)$, we can obtain the averages of various powers of ΔE_0 , i.e.,

$$\tilde{M}_n = \left. \frac{d^n G(u, \tau)}{du^n} \right|_{u=0} = (-i)^n \langle (\Delta E_0)^n \rangle. \quad (16)$$

Since \tilde{M}_n are related to the LCs of the u evolution, below we relate these averages with \tilde{a}_n and \tilde{b}_n .

Using the expression for $G(u, \tau)$ given in Eq. (8), we obtain the first two such averages to be equal to⁶

$$\begin{aligned} \langle \Delta E_0 \rangle &= \langle E_{00} | W_\tau^\dagger H_0 W_\tau | E_{00} \rangle \\ &= \langle E_{00}, \tau | H_0 | E_{00}, \tau \rangle \end{aligned} \quad (17)$$

and

$$\begin{aligned} \langle (\Delta E_0)^2 \rangle &= \langle E_{00} | [W_\tau, H_0]^\dagger [W_\tau, H_0] | E_{00} \rangle \\ &= \langle E_{00}, \tau | H_0^2 | E_{00}, \tau \rangle. \end{aligned} \quad (18)$$

Now from the identification between the moments of the CF and the LCs in a quench scenario made in [57], we obtain the first two LCs in terms of the above averages as

$$\tilde{a}_0 = \langle \Delta E_0 \rangle = \langle E_{00}, \tau | H_0 | E_{00}, \tau \rangle, \quad (19)$$

$$\begin{aligned} \tilde{b}_1^2 &= \langle (\Delta E_0)^2 \rangle - \langle \Delta E_0 \rangle^2 \\ &= \langle E_{00}, \tau | H_0^2 | E_{00}, \tau \rangle - \langle E_{00}, \tau | H_0 | E_{00}, \tau \rangle^2. \end{aligned} \quad (20)$$

Therefore, we see that \tilde{a}_0 is the average of the initial Hamiltonian H_0 in the initial state, while \tilde{b}_1^2 is the variance of ΔE_0 . Similar relations can also be established between the higher-order LC and various powers of averages of ΔE_0 . Analytical forms for these are complicated and, therefore, we do not present them here for brevity.

Here we also note that \tilde{b}_1 , in the form written above, is very similar to the Fubini-Study (FS) metric generated by H_0 from the initial state $|E_{00}, \tau\rangle$ of the circuit time evolution.⁷ This line element is the starting point of the definition of an alternative geometric notion of circuit complexity compared to that of Nielsen's [71–74], and is known as the FS complexity [75]. In this definition of the circuit complexity, one uses the FS line element defined on the space of pure states as a state-dependent measure of the cost function, and subsequently obtains the associated complexity between two states by finding out the geodesic distance between them as measured by

⁶As we have mentioned before, we have neglected an overall phase factor present in the CF during writing these formulas.

⁷More specifically, for each value of the circuit time, \tilde{b}_1 is equal to the FS metric.

the FS metric [76] (see also [77,78]).⁸ In a similar vein, we see that another state-dependent cost $F_{|\langle H_0 \rangle|} = |\langle E_{00}, \tau | H_0 | E_{00}, \tau \rangle|$ proposed in [82] is equal to the modulus of the LC \tilde{a}_0 , with the role of the instantaneous Hamiltonian played by H_0 .

The fact that \tilde{a}_0 and \tilde{b}_1 are related to the well-known cost functions in geometric approaches to the circuit complexity provides a possible way of connecting these measures of circuit complexity and the SC studied here. In principle, by using the reverse argument, one can define other new types of cost functions from other LCs as well, and study the resulting measures of circuit complexity. Therefore, we can conclude that it is possible to understand various cost functions as LCs with respect to some unitary evolution. Hopefully, this will shed new light on the connection between these two distinct measures of defining complexity of quantum systems.

D. Connection with the fidelity OTOC

Before moving on to the following sections, where we compute the SC of the u evolution and the associated quantities, here we discuss an interesting connection with the fidelity OTOC (FOTOC), a class of OTOCs, where one sets the operator V in Eq. (3), as the projector on the initial state [83]. This quantity can provide important insights into the scrambling of information in quantum many-body systems. Recently, in [84], this quantity has been studied for the Dicke model of quantum optics and it was shown there that FOTOCs can connect scrambling, volume law of the Renyi entropy, and thermalization. Specifically, here we show that for small values of the evolution parameter, the LC \tilde{b}_1 is related to the FOTOC.

The FOTOC is defined as (according to the notation used in this paper)

$$\mathcal{F}(t) = \langle O_0 | W_t^\dagger \rho(0) W_t \rho(0) | O_0 \rangle, \quad (21)$$

where $\rho(0) = |O_0\rangle\langle O_0|$ is the projector on the initial state, and W_t is the Heisenberg picture operator corresponding to W . To understand the significance of this quantity, we consider the modulus squared of the CF of the TPM protocol [given in Eq. (8)]

$$|G(u, \tau)|^2 = |\langle O_0 | W_\tau^\dagger e^{-iuO} W_\tau e^{iuO} | O_0 \rangle|^2. \quad (22)$$

With a little manipulation we can rewrite this as

$$|G(u, \tau)|^2 = \langle O_0 | \tilde{W}_t^\dagger \rho(0) \tilde{W}_t \rho(0) | O_0 \rangle = \mathcal{F}(t, u), \quad (23)$$

where $\tilde{W}_t = W_\tau^\dagger e^{iuO} W_\tau$. As the last identification indicates, this is just the FOTOC between the operators \tilde{W}_t and $V = \rho(0)$. Notice that $|G(u, \tau)|^2$ is also the modulus squared of the Fourier transform of the probability distribution of ΔO is a TPM protocol [see Eq. (4)], and it can also be written as the product of Fourier transforms of two probability distributions of two different TPMs, one for the measurement of the operator O (corresponding to the change of eigenvalue $\Delta O = O_n - O_0$), and the other for the measurement of the operator

$\tilde{O} = -O$ (and, hence, corresponding change of eigenvalue is $\Delta \tilde{O} = -\Delta O = O_0 - O_n$). Furthermore, from the expression for $|G(u, \tau)|^2$ in Eq. (22), we see that, when the OTOC of the TPM is interpreted as the ACF, the above FOTOC is also the survival probability of the initial state $|O_0, \tau\rangle$ under O evolution.

Using the survival probability in Eq. (22), we can find out the behavior of the FOTOC at large u by computing its long- u average

$$\bar{\mathcal{F}}(\tau) := \lim_{u \rightarrow \infty} \frac{1}{u} \int_0^u du \mathcal{F}(\tau, u). \quad (24)$$

Using the expression for $G(u, \tau)$ from Eq. (6) as well as Eqs. (5) and (4), we obtain this to be

$$\bar{\mathcal{F}}(\tau) = \sum_n |\langle O_n | W_\tau | O_0 \rangle|^4. \quad (25)$$

Therefore, here the long- u average of the FOTOC is just the sum of the square of the transition probabilities. Furthermore, noting that $|O_0, \tau\rangle = W_\tau |O_0\rangle$, we also see that $\bar{\mathcal{F}}(\tau)$ is just the IPR of the state $|O_0, \tau\rangle$ in the eigenbasis of the operator O (see Sec. VI below).

We can obtain an instructive behavior of the FOTOC for small values of u as well. For a TPM protocol where $O = H_0$, the FOTOC becomes the survival probability of the state $|E_{00}, \tau\rangle$ under the Hamiltonian evolution

$$\mathcal{F}(\tau, u) = |\langle E_{00}, \tau | e^{-iH_0 u} | E_{00}, \tau \rangle|^2, \quad (26)$$

so that, for $u \ll 1$, we can write it as

$$\begin{aligned} \mathcal{F}(\tau, u) &= 1 - u^2 (\langle E_{00}, \tau | H_0^2 | E_{00}, \tau \rangle - \langle E_{00}, \tau | H_0 | E_{00}, \tau \rangle^2) \\ &= 1 - u^2 \tilde{b}_1^2. \end{aligned} \quad (27)$$

Therefore, for small values of u , the FOTOC decays quadratically with u , and the decay rate is characterized by the LC \tilde{b}_1 . For this kind of quadratically decaying survival probability, it is known that the corresponding SC would grow quadratically with u [62].

We also notice that \tilde{b}_1 is equal to the quantum Fisher information of H_0 in the time-evolved state. Quantum Fisher information for a pure state is defined as the variance of H_0 [85], and is a central quantity in parameter estimation as well as a key witness for multipartite entanglement [86].

IV. SPREAD COMPLEXITY OF u EVOLUTION ASSOCIATED WITH LIE ALGEBRAS

In this section we analytically obtain the SC of the u -evolution by using some assumptions about the operator O and the Hamiltonians generating the time evolution. Specifically, we assume that O is an element of some Lie algebra, and use the analytical technique developed in [51,87] to obtain the Krylov basis and the SC that we have defined in Eq. (15). To complement these analytical computations, in the next section, we numerically obtain the SC for realistic spin systems in both integrable and chaotic cases. These examples will help us

⁸For works that use the related so-called quantum information metric to define the FS complexity in the parameter space of quantum many-body systems showing ground- and excited-state quantum phase transitions see [79–81].

to clearly understand various properties of the quantity $\mathcal{C}(\tau, u)$ we have introduced above.

A. The u -evolved state

Assuming that W is an unitary operator, we first write the ACF in Eq. (9) in the following way:

$$\begin{aligned} G(u, \tau) &= \langle O_0 | e^{-iW_{\text{ef}}(\tau)} e^{-iuO} e^{iW_{\text{ef}}(\tau)} | O_0 \rangle \\ &= \langle O_0 | e^{-iuO_{\text{ef}}(\tau)} | O_0 \rangle, \end{aligned} \quad (28)$$

where we have used the notation

$$W_\tau = e^{-iW_{\text{ef}}(\tau)} \quad \text{and} \quad O_{\text{ef}}(\tau) = e^{-iW_{\text{ef}}(\tau)} O e^{iW_{\text{ef}}(\tau)}. \quad (29)$$

As is evident from these relations, $W_{\text{ef}}(\tau)$ is a Hermitian operator which contains information of the time evolution of the operator W under the Hamiltonian H and, similarly, O_{ef} is also a Hermitian operator (since O is also Hermitian) which encodes the effect of $W_{\text{ef}}(\tau)$ on the observable O .

From Eq. (28) we see that $G(u, \tau)$ can be equivalently viewed as the ACF between the u -evolved state $e^{-iuO_{\text{ef}}} | O_0 \rangle$ and the initial state $| O_0 \rangle$. This is an alternative viewpoint from the one described in the previous section, with the most important difference between the two scenarios being that, in the present case, the initial state of the circuit time evolution is actually independent of the time (τ) when the perturbation is applied. In fact here, the initial state is just an eigenstate of the operator O . Even so, the u -evolved state is still nontrivial since the u evolution here is generated through the “effective” observable $O_{\text{ef}}(\tau)$ rather than O itself (unlike the previous scenario), and the operator $O_{\text{ef}}(\tau)$ now is time dependent (in the previous case the initial state was time dependent). This is the viewpoint we use throughout the present section and will return to the previous version in the next section, though we emphasize that both of them are equivalent (since they are just alternative ways of writing the same quantity, an OTOC), and which one has to be used is just a matter of convenience (we discussed this equivalence briefly in Appendix).

To proceed analytically, and to use the geometric method of obtaining the LCs and the Krylov basis developed in [51,87], we assume that the operators $W_{\text{ef}}(\tau)$ and O are of the form

$$W_{\text{ef}}(\tau) = \alpha f(\tau)(K_+ + K_-) = f(\tau)L \quad \text{and} \quad O = \gamma K_0, \quad (30)$$

where α and γ are two real constants, $f(\tau)$ is a real function of time, and the three operators K_i are assumed to be the generators of a Lie algebra. In this paper, we consider the cases when the Lie algebra under consideration is either $\text{su}(1, 1)$ or $\text{su}(2)$, so that the generators satisfy the following commutation relations:

$$[K_-, K_+] = 2\sigma K_0, \quad [K_0, K_\pm] = \pm K_\pm. \quad (31)$$

When σ is 1, the algebra generated by these operators is a $\text{su}(1, 1)$ algebra, while, for $\sigma = -1$ they become the generators of the $\text{su}(2)$ algebra. Note that we have assumed that the operator O is only proportional to K_0 . It is, of course, possible to take a more general form for both the operators W_{ef} and O

(e.g., a general combination of all three generators),⁹ however, for our purposes, this relatively simple form is sufficient.

To evaluate the final operator $O_{\text{ef}}(\tau)$, we need the expressions for the commutator $[L, O]$ as well as the higher-order nested commutators between L and $[L, O]$. From the definitions of L and O , we first obtain

$$[L, O] = \alpha\gamma(K_- - K_+) = \gamma\bar{L}, \quad [L, [L, O]] = -4\alpha^2\sigma O, \quad (32)$$

where, for convenience, we have renamed $\alpha(K_- - K_+)$ as \bar{L} . Similarly, all the higher-order nested commutators can be evaluated in terms of \bar{L} and O . Now using the Baker-Campbell-Hausdorff lemma, we can evaluate $O_{\text{ef}}(\tau)$ from Eq. (29) to be the following series:

$$\begin{aligned} O_{\text{ef}}(\tau) &= O \left[1 - \frac{f(\tau)^2}{2!} (-4\alpha^2\sigma) + \frac{f(\tau)^4}{4!} (-4\alpha^2\sigma)^2 + \dots \right] \\ &\quad - i\gamma\bar{L} \left[f(\tau) - \frac{f(\tau)^3}{3!} (-4\alpha^2\sigma) \right. \\ &\quad \left. + \frac{f(\tau)^5}{5!} (-4\alpha^2\sigma)^2 + \dots \right]. \end{aligned} \quad (33)$$

This series has different expressions for $\text{su}(2)$ and $\text{su}(1, 1)$ algebras. For the $\text{su}(2)$ algebra (for which $\sigma = -1$), taking $\gamma = 2\alpha$ we can sum the above series and write the final expression in a compact form as

$$O_{\text{ef}}(\tau) = O \cos[2\alpha f(\tau)] - i\bar{L} \sin[2\alpha f(\tau)]. \quad (34)$$

On the other hand, for the $\text{su}(1, 1)$ algebra (for which $\sigma = 1$), once again taking $\gamma = 2\alpha$, we arrive at the following expression for the “effective observable” operator:

$$O_{\text{ef}}(\tau) = O \cosh[2\alpha f(\tau)] - i\bar{L} \sinh[2\alpha f(\tau)]. \quad (35)$$

From these expressions for the effective operator $O_{\text{ef}}(\tau)$, we see that for both the Lie algebras under consideration, this is a general element of the respective algebra and, therefore, can be written in the following general form:

$$O_{\text{ef}}(\tau) = \mathcal{A}_0(\tau)K_0 + i\mathcal{A}_1(\tau)(K_+ - K_-), \quad (36)$$

where the τ -dependent coefficients $\mathcal{A}_0(\tau)$ and $\mathcal{A}_1(\tau)$ can be read off from Eqs. (34) and (35). For the $\text{su}(2)$ algebras, these are given by

$$\mathcal{A}_0 = 2\alpha \cos[2\alpha f(\tau)], \quad \mathcal{A}_1 = \alpha \sin[2\alpha f(\tau)], \quad (37)$$

while for the $\text{su}(1, 1)$ algebra we have

$$\mathcal{A}_0 = 2\alpha \cosh[2\alpha f(\tau)], \quad \mathcal{A}_1 = \alpha \sinh[2\alpha f(\tau)]. \quad (38)$$

B. The Lanczos coefficients and the Krylov basis

For the u evolution of Eq. (28), the operator O_{ef} plays the role of the Hamiltonian, and the corresponding Krylov basis vectors are generated by the action of this operator on the

⁹In that case, the Krylov basis would not simply be the basis states of the representation of the Lie algebra (or at most related through some phase factor, as is the case below), rather would be given by linear combinations of them.

initial state $|O_0\rangle$. As we have discussed at the beginning of this section, though the interpretation of the ACF of (8) used in the present section is slightly different from the previous section, for convenience, we still denote the Krylov basis and the LC with tildes to distinguish them from those corresponding to the Hamiltonian evolution. In particular, with the notation we use here, the action of the operator O_{ef} on the Krylov basis is of the form

$$O_{\text{ef}}|\tilde{K}_n\rangle = \tilde{a}_n|\tilde{K}_n\rangle + \tilde{b}_{n+1}|\tilde{K}_{n+1}\rangle + \tilde{b}_n|\tilde{K}_{n-1}\rangle. \quad (39)$$

Now since $O_{\text{ef}}(\tau)$ is an element of a Lie algebra, the u -evolved state $|\Psi(u)\rangle = e^{-iuO_{\text{ef}}}|O_0\rangle$ is a generalized or Perelomov coherent state (CS) associated with $\text{SU}(2)$ [or $\text{SU}(1, 1)$] Lie group [88]. Therefore, we can use the geometrical method based on the generalized CS developed in [51,87] to directly obtain the Krylov basis and the associated LCs. We obtain these separately for the two algebras under consideration.

Case 1: the $\text{su}(2)$ algebra. First, we specify the action of the generators of $\text{su}(2)$ algebra on the basis for representation $|j, -j+n\rangle$. These are given by the standard formulas¹⁰

$$\begin{aligned} K_0|j, -j+n\rangle &= (-j+n)|j, -j+n\rangle, \\ K_+|j, -j+n\rangle &= \sqrt{(n+1)(2j-n)}|j, -j+n+1\rangle, \\ K_-|j, -j+n\rangle &= \sqrt{n(2j-n+1)}|j, -j+n-1\rangle, \end{aligned} \quad (40)$$

where $j = 0, 1/2, 1, \dots$ and $n = 0, 1, \dots, 2j$. Furthermore, the conditions $K_+|j, j\rangle = 0$, and $K_-|j, -j\rangle = 0$ are satisfied. Here we assume that the initial state $|O_0\rangle$ is the state $|j, -j\rangle$ and, therefore, is annihilated by the operator K_- .

Now comparing the action of the operator O_{ef} on the states $|j, -j+n\rangle$ of the above representation [using the relations in Eqs. (40)], and comparing with the definition of the Krylov basis in Eq. (39), we get the elements of the Krylov basis and the LCs in this case to be

$$\begin{aligned} |\tilde{K}_n\rangle &= i^{n+1}|j, -j+n\rangle, \quad \tilde{a}_n = \mathcal{A}_0(n-j), \\ \tilde{b}_n &= \mathcal{A}_1\sqrt{n(2j-n+1)}, \end{aligned} \quad (41)$$

where, from Eq. (34) we get the coefficients $\mathcal{A}_0 = 2\alpha \cos[2\alpha f(\tau)]$ and $\mathcal{A}_1 = \alpha \sin[2\alpha f(\tau)]$. Notice the extra phase factor of i^{n+1} in front of the element of the Krylov basis above, which usually remains absent from the Krylov basis generated by the Hamiltonian evolution [51]. This is due to the minus sign between the operators K_+ and K_- in the expression for O_{ef} , and does not have any effect in the SC.

Case 2: $\text{su}(1, 1)$ algebra. In this case the action of the generators on the basis of representation $|h, n\rangle$ are given by

the following relations:

$$\begin{aligned} K_0|h, n\rangle &= (h+n)|h, n\rangle, \\ K_+|h, n\rangle &= \sqrt{(n+1)(2h+n)}|h, n+1\rangle, \\ K_-|h, n\rangle &= \sqrt{n(2h+n-1)}|h, n-1\rangle, \end{aligned} \quad (42)$$

here n is a non-negative integer, and the constant h is called the Bargmann index. It is well known that, for a single-mode bosonic representation of $\text{su}(1, 1)$ algebra, the Bargmann index can take values $\frac{1}{4}$ or $\frac{3}{4}$ (see, e.g., [90]). In this paper, we assume that the basis corresponding to a unitary irreducible representation of the $\text{su}(1, 1)$ Lie algebra is a set of states which contains an even number of bosons, so that h is taken to be $\frac{1}{4}$. Here we also assume that the initial state is $|O_0\rangle = |h, 0\rangle$.

Once again, considering the action of the operator $O_{\text{ef}}(\tau)$ on the basis $|h, n\rangle$, using Eqs. (42), and comparing the result with the definition in Eq. (39), we obtain the Krylov basis and LCs to be

$$\begin{aligned} |\tilde{K}_n\rangle &= i^{n+1}|h, n\rangle, \quad \tilde{a}_n = \mathcal{A}_0(n+h), \\ \tilde{b}_n &= \mathcal{A}_1\sqrt{n(2h+n-1)}, \end{aligned} \quad (43)$$

where from Eq. (35) we now have $\mathcal{A}_0 = 2\alpha \cosh[2\alpha f(\tau)]$, and $\mathcal{A}_1 = \alpha \sinh[2\alpha f(\tau)]$.

Since the LCs are dependent on τ through the coefficients \mathcal{A}_0 and \mathcal{A}_1 , it is instructive to compare the magnitudes of LC for different fixed values of $\tau = \tau_i$.¹¹ For the $\text{su}(2)$ algebra, the LC changes periodically with $\bar{\tau} = f(\tau)$, while for the $\text{su}(1, 1)$ algebra they grow with $\bar{\tau}$, with the growth being exponential for large values of $\bar{\tau}$. Furthermore, for large $\bar{\tau}$, the growth rates of both sets of coefficients \tilde{a}_n and \tilde{b}_n with respect to $\bar{\tau}$ are equal and are fixed by the constant α .

C. Evolution of spread complexity

Using the LCs obtained above, we now find out the SC of the u evolution defined in Eq. (15). Here, we shall show the computation of SC only for the $\text{su}(1, 1)$ algebra, and an entirely similar procedure can be followed to find out the SC for the $\text{su}(2)$ algebra.

First we use the decomposition formula for the $\text{su}(1, 1)$ algebra (see, e.g., [89]) to write the u -evolved state in the form (using $h = \frac{1}{4}$)

$$\begin{aligned} |\Psi(u)\rangle &= \exp(C_+K_+)\exp(C_0K_0)\exp(C_-K_-)|h, 0\rangle \\ &= (C_0)^{1/4} \sum_{n=0}^{\infty} \frac{1}{n!} (C_+)^n (K_+)^n |h, 0\rangle, \end{aligned} \quad (44)$$

where C_{\pm} , C_0 are functions of τ and u , and are given by the expressions

$$C_{\pm}(\tau, u) = \frac{c_{\pm}(\tau, u)}{g(\tau, u)\Theta(u)} \sinh \Theta(u), \quad C_0(\tau, u) = g(\tau, u)^{-2}, \quad (45)$$

¹⁰To be consistent with the notations used in [87], we have shifted $n \rightarrow j+n$ from the usual convention, e.g., the one used in [89] to derive the decomposition formulas associated with the $\text{su}(2)$ Lie algebra.

¹¹We analyze a similar setting numerically in the next section, where the different values τ fix the initial state of the u evolution. Here, the values of τ change the coefficients of the generators in the operator $O_{\text{ef}}(\tau)$ generating the u evolution with respect to the initial state $|O_0\rangle$.

with

$$\begin{aligned} g(\tau) &= \cosh \Theta(u) - \frac{c_0(\tau, u)}{2\Theta(u)} \sinh \Theta(u), \\ c_+ &= -c_- = u\alpha \sinh[2\alpha f(\tau)], \\ c_0 &= -2iu\alpha \cosh[2\alpha f(\tau)], \\ \Theta(u) &= \left[\left(\frac{c_0}{2} \right)^2 - c_+ c_- \right]^{1/2} = iu\alpha. \end{aligned} \quad (46)$$

From the above expression for the evolved state we get the simplified expression for the ACF to be $\mathcal{S}(u) = \langle \Psi(u) | h, 0 \rangle = [C_+(\tau)]^{1/4}$, and comparing the expansion in second line above with the expansion in Eq. (13) of an arbitrary u -evolved state in the Krylov basis we obtain

$$\begin{aligned} \tilde{\phi}_n(\tau, u) &= \mathcal{N}_n [C_0(\tau, u)]^{1/4} [C_+(\tau, u)]^n, \\ \text{where } \mathcal{N}_n &= i^{-(n+1)} \sqrt{\frac{\Gamma(n + \frac{1}{2})}{n! \sqrt{\pi}}}. \end{aligned} \quad (47)$$

Using these expressions for $\tilde{\phi}_n(\tau, u)$, we can perform the summation in Eq. (15) exactly, and the resulting expression for the SC of u evolution can be compactly written as [51,57]

$$\begin{aligned} \mathcal{C}(\tau, u) &= \frac{|\tilde{\phi}_1(\tau, u)|^2}{[1 - F(\tau, u)]^{3/2}}, \\ \text{where } F(\tau, u) &= |C_+(\tau, u)|^2. \end{aligned} \quad (48)$$

V. SPREAD COMPLEXITY OF u EVOLUTION IN INTEGRABLE AND CHAOTIC SYSTEMS

In this section we numerically study the SC of circuit evolution for different integrable and chaotic interacting quantum systems using the following return amplitude:

$$\begin{aligned} G(u, \tau) &= \langle E_0 | W_\tau^\dagger e^{-iH_0 u} W_\tau | E_0 \rangle \\ &= \langle E_0, \tau | e^{-iH_0 u} | E_0, \tau \rangle, \end{aligned} \quad (49)$$

where W is some local operator acting on $|E_0\rangle$, a bulk eigenstate of H_0 , and $W_\tau = e^{-iH_1 \tau} W e^{iH_1 \tau}$ is the Heisenberg operator at time τ evolved through the postquench Hamiltonian H_1 . Therefore, the observable O that one measures in the TPM protocol is the Hamiltonian H_0 of the system before $t < 0$. This is the case we considered in Sec. III C to understand the significance of the LC. Notice that, since here H_0 is a Hamiltonian, the parameter u can be thought of as the Fourier conjugate of the eigenvalues of H_0 . In fact, in the absence of the perturbation W , the resulting ACF would just represent the time evolution of an eigenstate of H_0 . The presence of the perturbation changes the initial state $|E_0\rangle$ nontrivially, so that finding the spreading under evolution generated by H_0 has a well-defined meaning, as it carries the implications of the perturbation W in the evolution of the TPM protocol.

Here we take H_0 and H_1 to be the integrable or chaotic limit of the Ising chain with different combinations, as we describe below. In all the cases considered below, we take the perturbation W to be $W = e^{-i\theta \sigma_z}$ with $\theta = \pi/2$. The explicit form for the Hamiltonians we consider are the following:

$$H_{\text{int}}(J, h) = - \sum_{i=1}^N [J \sigma_{i+1}^z \sigma_i^z + h \sigma_i^x] \quad (50)$$

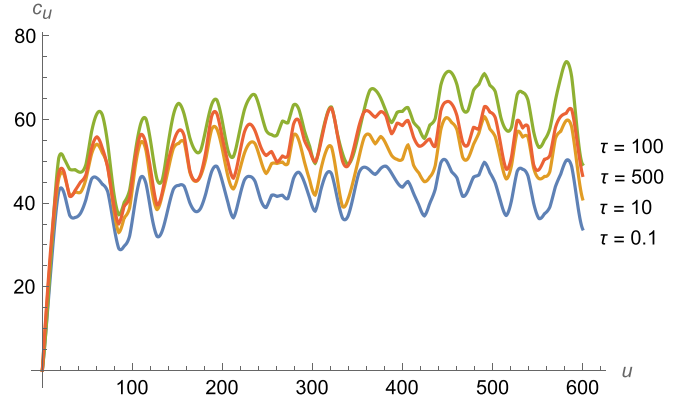


FIG. 2. SC of the u evolution when both H_0 and H_1 are integrable, for different fixed values of the parameter τ , which fixes the initial state. Here, $H_0 = H_{\text{int}}(1, 0.4)$ and $H_1 = H_{\text{int}}(1, 0.7)$, respectively.

and

$$H_{\text{cha}}(J, h, g) = - \sum_{i=1}^N [J \sigma_{i+1}^z \sigma_i^z + h \sigma_i^x + g \sigma_i^z], \quad (51)$$

where the σ_i are the Pauli matrices at the i th site of the chain. In the first case, $g = 0$, and the Hamiltonian is that of an Ising model with a transverse field and is integrable [91]. On the other hand, in the second case, with nonzero values of both the parameters g and h , the Hamiltonian is nonintegrable, as can be verified by finding out the level spacing distribution of $H_{\text{cha}}(J, h, g)$, which in this case is close to the Wigner-Dyson distribution characterizing a chaotic system [92]. In all the cases considered below, we take $N = 12$. The chosen parameter values are indicated in the captions of Figs. 2–4.

Case 1. First we consider the case when both H_0 and H_1 are taken as integrable Hamiltonians. In this case the SC, $\mathcal{C}(\tau_i, u)$ [defined in Eq. (15) above] for different fixed values of $\tau = \tau_i$, are plotted in Fig. 2. As we have explained in Sec. III B above, these values of τ fix the initial state $|O_0, \tau\rangle$ of the u evolution. In the TPM protocol, the parameter τ denotes the time when the perturbation W is applied and, therefore, starting from the lower values of τ , its increasing values indicate that the

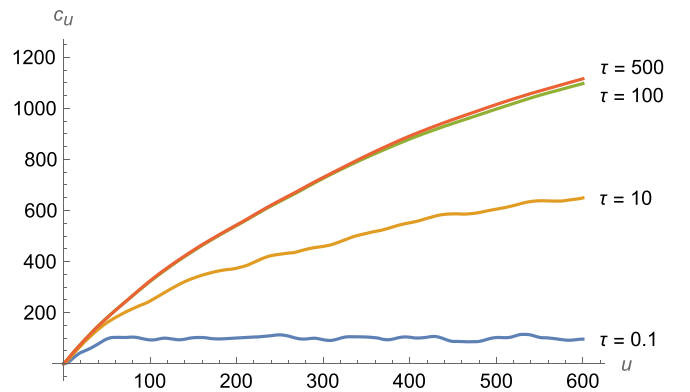


FIG. 3. SC of the circuit evolution for different values of τ , when H_0 is integrable and H_1 is chaotic. Here, $H_0 = H_{\text{int}}(1, 0.4)$ and $H_1 = H_{\text{cha}}(1, 1.4, -0.6)$.

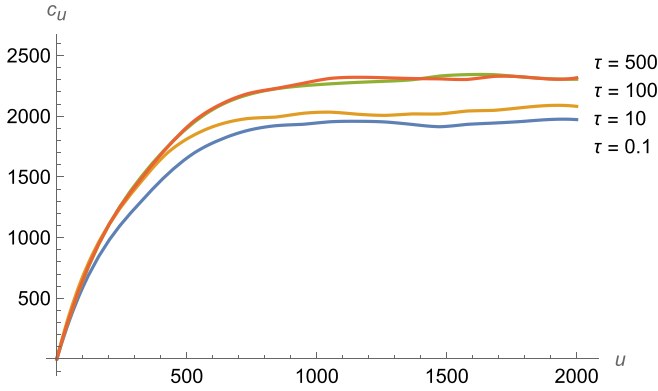


FIG. 4. SC of the circuit evolution for different values of τ , when H_0 and H_1 both chaotic. Here, $H_0 = H_{\text{cha}}(0.8, 1.2, -0.6)$ and $H_1 = H_{\text{cha}}(1, 1.4, -0.6)$.

initial state $|O_0, \tau\rangle$ gets more and more complicated with τ . Furthermore, how this state changes with time is encoded in the time-evolved operator W_τ , and a useful measure of this is the operator complexity C_W of the perturbation operator W .

From Fig. 2 we observe that $C(\tau_i, u)$ does not have a prominent growth at early times and does not show saturation, even for large values of u . Similarly, from the plots of $C(\tau_i, u)$ for different values of τ_i , we see that, as one varies τ , even for large τ , the SC does not attain steady behavior. These features of SC evolution can be attributed to the fact that H_0 , generating the circuit time evolution is integrable, so that the SC shows the usual oscillatory behavior observed for an integrable Hamiltonian.

Case 2. Next, we consider the case when H_0 is the integrable Hamiltonian of Eq. (50), and H_1 is the chaotic one given in Eq. (51). In this case we plot $C(\tau_i, u)$ for different values of τ in Fig. 3. Comparing with Fig. 2 (where H_1 was taken as integrable) we see that, in this case the initial growth of the SC is more prominent, and the differences in the magnitudes of $C(\tau_i, u)$ for different values τ_i are greater (until at later times, when the operator complexity of W saturates and initial states for different large values of τ are similar). This can be understood from the fact that here the postquench Hamiltonian H_1 , which determines the initial state of the u evolution, is in fact a chaotic one, so that even for small values of τ , the initial states are quite different from each other. On the other hand, at later times τ_i , the profiles of $C(\tau_i, u)$ are quite similar, since H_1 being chaotic, the W evolution gets saturated at these values of τ_i . Thus, the pattern of SC for different τ occurs due to the differences in growth of the perturbation operator W under chaotic and integrable dynamics in the present case and in case 1, discussed in the previous paragraph. This is reflected in the dependence of \tilde{b}_1 on OTOC and fidelity OTOC (discussed at the end of Sec. III). Furthermore, in this case, H_0 being integrable, the SC keeps oscillating even for higher values of u .

Case 3. Finally, we consider the case when both H_0 and H_1 are chaotic, and the evolution of the SC with respect to u for different fixed values of τ are shown in Fig. 4. In this case, we see that the SC shows prominent linear growth of small values of u and saturation at large values u , and there is a peak

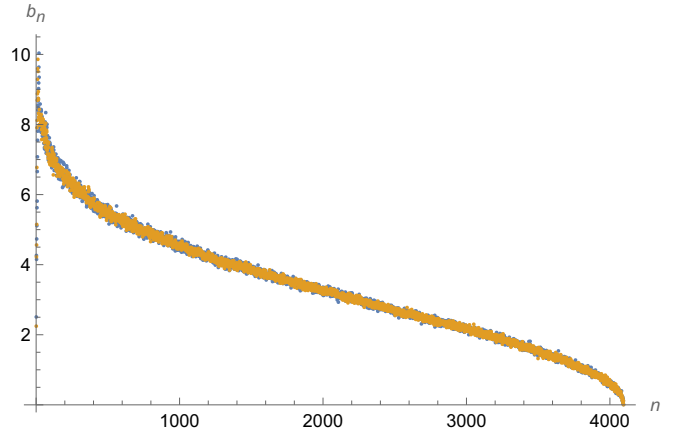


FIG. 5. Plot of the second set of LCs (b_n) for different values of τ , when H_0 and H_1 are both chaotic. The blue points are with $\tau = 0.1$, and the yellow points are with $\tau = 500$. All other parameters are the same as in Fig. 4.

in-between.¹² These features are consistent with the behavior of time evolution of the SC for interacting chaotic systems after sudden quenches [62]. We also notice that the peak in the SC is present irrespective of the values of τ , i.e., the initial state.

It can also be seen that, similar to the observation made in case 2, for large values of τ , the SC profiles almost merge into each other. This can once again be explained by noting that the initial state $|O_0, \tau\rangle$, with fixed values of τ , is fixed by the chaotic Hamiltonian H_1 in both the cases. Furthermore, the difference between Figs. 3 and 4 is also clear from the respective plots. When H_0 is chaotic, the linear growth of the SC continues up to long times compared to when H_0 is integrable, and in the latter case the SC profile shows oscillations even at late u values, whereas in the first case, the oscillations dry out quickly. In Fig. 5, we have also plotted the behavior of the second set of LCs (b_n) for two different values of τ , i.e., for two different initial states of the u evolution. The pattern for the b_n follows the usual behavior of b_n 's for a chaotic Hamiltonian [51]. Furthermore, due to the chaotic nature of the Hamiltonian H_1 , the sets of b_n 's for two different initial states are almost identical [as can also be seen by plotting the histogram of $\log(b_n/b_{n+1})$], so that the corresponding SC profiles are also almost identical.

From the discussion of the three cases, we see that only when the Hamiltonian H_0 generating the circuit time evolution is chaotic, the SC saturates at large values u . However, the postquench Hamiltonian H_1 also has important effects on u evolution through the initial state, and depending on whether it is integrable or chaotic, the SC profile for different τ can be different. In particular, when H_1 is chaotic, for higher values of τ , the magnitudes of the SC are almost equal, even though

¹²The peak is not clearly visible from the plots shown in Fig. 4, due to the fact that the dip (also called the correlation hole) in the corresponding survival probability is not prominent. This behavior is similar to the one shown by time evolution of the SC in interacting realistic spin chains [62].

they can oscillate or saturate, depending on whether H_0 is integrable or chaotic.

VI. INVERSE PARTICIPATION RATIO AND THE LANCZOS COEFFICIENTS

In this section, we discuss an interesting connection between the IPR and the LCs. As shown in [60], the initial growth of SC is not sensitive to whether the system Hamiltonian is chaotic or integrable. Here we show that the early evolution of the SC can actually be explained from the behavior of the IPR of the state $|O_0, \tau\rangle$ in the eigenstates of the O operator. We compute the IPR and the first few LCs when H_1 is taken as an element of the $\text{su}(1, 1)$ algebra.

We consider a Lie algebraic model similar to the one discussed in Sec. IV; however, here we explicitly specify the form for the system Hamiltonians to be $H_0 = K_0$ and $H_1 = \alpha(K_+ + K_-) + K_0$, where the K_i are the generators of $\text{su}(1, 1)$ algebra, and α is a real constant. Furthermore, we assume the perturbation operator to be $W = \exp[i(K_+ + K_-)]$. We first want to compute the time-evolved Heisenberg picture operator $W_\tau = e^{-iH_1\tau} W e^{iH_1\tau}$. This can be easily done by repeatedly applying $\text{su}(1, 1)$ decomposition formulas [89] to get a decomposition of W_τ of the form

$$e^{-iH_1\tau} W e^{iH_1\tau} = \exp(A_+ K_+) \exp[\ln(A_0) K_0] \times \exp(A_- K_-). \quad (52)$$

It is possible to write the exact analytical formulas for the functions $A_i(\tau)$. However, these are extremely complicated, and we do not show them here.

We are also interested in finding out the IPR of the state $|O_0, \tau\rangle$ in terms of the eigenstates of H_0 . For the above choice of the Hamiltonian H_0 , this is given by the formula

$$\text{IPR} = \sum_{n=0}^{\infty} |\langle h, n | O_0, \tau \rangle|^4. \quad (53)$$

The IPR is a measure for the level of delocalization of an initial state: a small value of IPR indicates that the initial state is delocalized in the basis $|h, n\rangle$. It is used to verify whether the local density of states [which is a quantity very similar to the quantity $P(\mathcal{W})$, the probability distribution of work done in a quench] of a many-body Hamiltonian is ergodically filled or not [91].

Assuming that the state after first measurement is $|h, 0\rangle$ (with $h = \frac{1}{4}$, as before), and using the decomposition in Eq. (52) above, we have the expression for $|O_0, \tau\rangle$ to be

$$\begin{aligned} |O_0, \tau\rangle &= \exp(A_+ K_+) \exp[\ln(A_0) K_0] |h, 0\rangle \\ &= (A_0)^{1/4} \sum_{n=0}^{\infty} \frac{(A_+)^n}{n!} (K_+)^n |h, 0\rangle, \end{aligned} \quad (54)$$

so that the IPR is given by the summation

$$\text{IPR} = \sum_{n=0}^{\infty} |\mathcal{N}_n[A_0(\tau)]^{1/4} [A_+(\tau)]^n|^4. \quad (55)$$

Using the analytical expressions for the functions $A_i(\tau)$, the IPR can be obtained for different values of the constant α as function of τ .

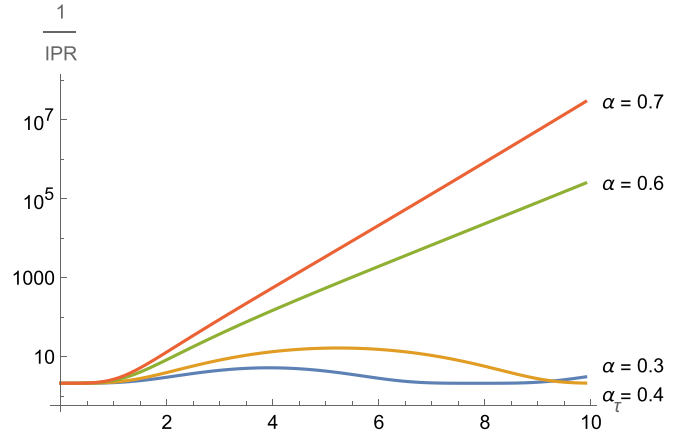


FIG. 6. Plot of the participation ratio $\frac{1}{\text{IPR}}$ for different fixed values of the constant α appearing in H_1 . Clearly, the behavior of $\frac{1}{\text{IPR}}$ changes from oscillatory to exponentially growing when α crosses the value 0.5.

Next we compute the LCs in this model by using the ACF

$$G(u, \tau) = \langle h, 0 | W_\tau^\dagger e^{-iH_0 u} W_\tau | h, 0 \rangle. \quad (56)$$

To calculate the ACF, we can follow a similar approach as above, and consider the following decomposition:

$$\begin{aligned} W_\tau^\dagger e^{-iH_0 u} W_\tau &= \exp(B_+ K_+) \exp[\ln(B_0) K_0] \\ &\times \exp(B_- K_-), \end{aligned} \quad (57)$$

where the functions $B_i(u, \tau)$ are now functions of both u and τ . Once again, their analytical expressions are complicated to provide here. In terms of these functions, the expression for the ACF simplifies to

$$\begin{aligned} G(u, \tau) &= \langle h, 0 | \exp[\ln(B_0(u, \tau)) K_0] | h, 0 \rangle \\ &= B_0(u, \tau)^{1/4}. \end{aligned} \quad (58)$$

Using this expression for the ACF we can calculate all the LCs recursively [51]. However, since the expressions for B_- , B_0 , and B_+ are complicated, it is only feasible to compute the first few LCs. These LCs are sufficient for our discussions below.

We now compare the behavior of IPR and LCs obtained above as functions of τ for different values of α . In Figs. 6 and 7 we have plotted the participation ratio ($\text{PR} = 1/\text{IPR}$), and the LC \tilde{b}_1 for different fixed values of α below and above 0.5. From these plots we observe that $\frac{1}{\text{IPR}}$ and \tilde{b}_1 show oscillatory behavior whenever α is less than 0.5 (indicating H_1 is stable), whereas, whenever α is greater than 0.5, both $\frac{1}{\text{IPR}}$ and \tilde{b}_1 show exponential growth with τ . This definitive change in the behavior of the LCs and the IPR can be explained mathematically by noticing that, from the decomposition formulas, the quantity that determines the behavior of the functions A_i and B_i is $\sqrt{\alpha^2 - \frac{1}{4}}$ (this quantity actually appears as the argument of cosine and sine functions). Therefore, when α crosses 0.5, all the oscillating terms become hyperbolic, resulting in the growth of IPR and LCs. Physically, this growth is due to the difference in the ability of the W_τ to spread the initial state over all the eigenstates of H_0 , i.e., coherence generating power, as discussed in [93]. This connection shows that in this scheme, the initial growth of the SC is sensitive to the

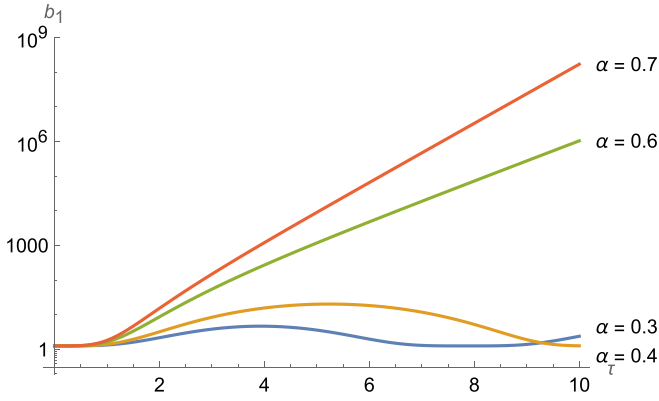


FIG. 7. Plot of the first LC \tilde{b}_1 for different fixed values of the constant α appearing in H_1 . Similar to the $\frac{1}{\text{IPR}}$, \tilde{b}_1 also shows transition from oscillatory to exponentially growing behavior when α crosses the value 0.5.

nature of H_1 . Here, we have illustrated this connection by considering H_1 as an element of a Lie algebra; however, it will be interesting to see whether this conclusion is true for realistic quantum chaotic systems as well.

VII. SUMMARY AND CONCLUSIONS

In this paper we have extended the concept of complexity of unitary evolution to the cases when an arbitrary initial state in a TPM protocol evolves under a backward and forward evolution through a Hamiltonian, with a perturbation applied in-between. Therefore, this quantity measures how an initial eigenstate of a Hermitian operator O spreads in the Hilbert space corresponding to a hypothetical system whose Hamiltonian is the operator O , i.e., it is the complexity of the u evolution, where the parameter u is the Fourier conjugate to the eigenvalues of the observable O , also known as the second time of evolution in the literature. As we have argued here, this definition of the SC of the u -evolved state is, in a sense, a bit different from the usual SC of a time-evolved state under a Hamiltonian evolution since here, the initial state (or, in a different interpretation, the generator of the circuit evolution) is determined the time-evolved perturbation operator W by a system Hamiltonian H . Thus, the nature of this perturbation W , as well as the Hamiltonian H , also play crucial roles in determining the SC of the u -evolved state. Hence, as we have verified in the numerical examples in Sec. V, the complexity of the u -evolved state incorporates both the operator complexity or the KC of the perturbation W (through the initial state), as well as the SC under the u evolution. For a sudden quench scenario, the one we have considered in this paper, the Hamiltonian H is the postquench Hamiltonian H_1 of a quantum system, whereas the operator O is the prequench Hamiltonian H_0 .

Our starting point has been an identification made in [8], where it was shown that the CF of the probability distribution of the difference in the eigenvalues of an operator O measured in a TPM protocol is the OTOC between the time-evolved (Heisenberg picture) perturbation operator W and the exponential of the operator O itself. Here, we have first identified this OTOC as the ACF corresponding to the

u evolution. Then, as the next natural step, we have studied the spread of an initial state under this dual or second time of evolution (also referred to as the circuit time in this paper to distinguish it from the usual time associated with evolution by the system Hamiltonian). The motivation for this has been the well-known fact that (the complex conjugate of) the ACF is the first coefficient among a set of probability amplitudes when a unitarily evolved state is written in terms of the Krylov basis generated by the corresponding generator of the unitary evolution. Furthermore, we have shown that, when O is the Hamiltonian H_0 , one can actually identify the LCs associated with the u evolution with certain state-dependent cost functions, such as the FS metric defined on the space of pure state. These relations, on one hand, provide clearer interpretations of these coefficients, while on the other hand show that it might be possible to directly make connections between SC and geometric measures of circuit complexity of a unitarily evolved state.¹³

In the latter part of this paper, we have used this definition of the SC to study the evolution of states with respect to the circuit time in both analytical and numerical examples, and illuminated new relationships between different well-known information-theoretic quantities, such as the FOTOC and the quantum Fisher information. The analytical example we have studied uses the Lie algebraic CS method of obtaining the Krylov basis, LCs as well as the SC. For the $\text{su}(1, 1)$ and $\text{su}(2)$ Lie algebras, we have shown how to obtain the LCs and the Krylov basis corresponding to the unitary evolution generated by the observable O .

The next example we have considered is that of a TPM protocol with a sudden quench, where the backward and forward time evolution is generated by a postquench Hamiltonian H_1 , whose parameters are different from those of the prequench Hamiltonian H_0 . Furthermore, H_0 is taken as the observable O , so that the circuit evolution (or the u evolution) is generated by H_0 itself. The quantum many-body system we consider is the integrable and the chaotic limits of an Ising chain in the presence of a transverse field, and for different values of the parameter τ (which fixes the initial state of the circuit evolution), we numerically obtain the SC of the state generated by H_0 . From the results we obtain it can be concluded that, only when H_0 is chaotic, the SC saturates at late circuit time. On the other hand, when H_1 is chaotic, it affects the SC of large τ initial states: namely, for this case, the magnitudes of the profile for the SC are identical.

Before concluding, here we outline some further implications of the results presented in our paper, as well as some important future directions that can be perused. First, the complexity of the spread of an initial state with respect to u evolution, that we have introduced here, can be thought of to be associated with a hypothetical auxiliary system whose

¹³In this context, we note that in a very recent work [94], the authors have shown that SC is not a measure of distance. Thus, unlike Nielsen's or FS complexity, the SC of a time-evolved state can not be understood as a geodesic distance between two points on some metric space. It will be interesting to find out the implications of this result in view of the above-mentioned connection between the LCs and certain cost functions for Nielsen's complexity geometry.

evolution is generated by the observable measured in the TPM protocol (and the role of time is played by the parameter conjugate to the eigenvalues of the observable). Since the ACF in such a system is the Fourier transform of the probability distribution of this observable, it is natural to ask what could be the quantity that is conjugated to the SC? Since one can write a Hermitian operator corresponding to SC, one way to approach this problem is to study the statistics of the SC itself and then consider the Fourier transform of that quantity. For chaotic or integrable Hamiltonians, this distribution should contain important information about the nature of these systems [11,70].

Second, the statistics of SC, as mentioned above, also points out a possible connection of the results discussed in this paper with experimentally measurable quantities. First, we notice that if we want to measure the statistics of work done on (or by) a system in a certain process, we need to keep track of the transitions between energy levels of the system before and after the process. This is of course true for measuring statistics of some other observable as well, i.e., we have to analyze the change in the eigenvalues of that observable before and after a process [see the definition of distribution for a general observable in a TPM scheme, Eq. (4)]. Though, for a generic quantum many-body system, keeping track of transitions between energy levels due to a nonequilibrium process (such as a quantum quench) is extremely difficult, for relatively simple quantum systems, the probability distribution of the work done has actually been measured in experimental setups, such as trapped atoms and ultracold atoms (see Refs. [95–97] for discussions on such experiments). From such measured WD, one can directly obtain the corresponding CF by using the Fourier transform of this distribution (in fact, this was the scheme proposed in [8] to measure OTOCs without using any ancillary systems), as well as LCs (see [57]). Now, since CF is the first of the set of coefficients $\tilde{\phi}_n$, we can, in turn, study Fourier transforms of the higher order $\tilde{\phi}_n$ as well, not only just $\tilde{\phi}_0$, and see whether those Fourier transforms have some physical meaning in a TPM protocol and whether these can be measured in experimental setups mentioned above which are used to measure the WD. Furthermore, since the SC is just the weighted sum of the modulus square of $\tilde{\phi}_n$'s, we believe it might provide a way of measuring SC itself from such experiments. Finding out the significance of Fourier transforms of each ϕ_n as a possible distribution of some quantum mechanical observable, and understanding their subsequent experimental significance is an interesting problem, and we hope to report on this in the future.

ACKNOWLEDGMENT

The work of T.S. is supported in part by the USV Chair Professor position at the Indian Institute of Technology, Kanpur.

APPENDIX: EQUIVALENCE OF DIFFERENT INTERPRETATIONS OF THE OTOC IN A TPM PROTOCOL

In Secs. III, IV, and V, we interpreted the OTOC in Eq. (8) as ACF in two different ways. In particular, in the interpretation used in Sec. III to define the SC of the u evolution, as well as in the numerical computations we did in

Sec. V, the circuit evolution is generated by the operator O itself, while the initial state it acts on depends on τ , the time after which the perturbation is applied in a TPM protocol through the operator W_τ . We call this the case 1. On the other hand, in Sec. IV, the u evolution is generated by an “effective” observable $O_{\text{ef}}(\tau)$, which itself is dependent on τ , and is determined the Hamiltonian H_1 as well as the perturbation W , while the initial state on which this evolution operator acts is itself independent of τ . This is designated as case 2 below. In this Appendix, we briefly discuss the relationship between the SC in these two cases and show that, in fact, the complexities defined in these two ways are equal: we can use any of them without affecting the physical conclusions.

First we write the u -evolved state in two cases (W_τ is Heisenberg picture time-evolved version of the unitary perturbation operator W),

$$\begin{aligned} |\Psi^1(u)\rangle &= e^{-iuO}|O_0, \tau\rangle = e^{-iuO}W_\tau|O_0\rangle, \text{ and} \\ |\Psi^2(u)\rangle &= e^{-iuO_{\text{ef}}}|O_0\rangle = W_\tau^\dagger e^{-iuO}W_\tau|O_0\rangle. \end{aligned} \quad (\text{A1})$$

Both of these evolved states can be expanded in terms of the Krylov basis generated by the operators O and O_{ef} , respectively, so that we have¹⁴

$$|\Psi^i(u)\rangle = \sum_n \tilde{\phi}_n^i(u)|\tilde{K}_n^i\rangle, \quad i = 1, 2. \quad (\text{A2})$$

Furthermore, comparing the two evolved states in Eq. (A1), we see that they are related by the unitary transformation $|\Psi^2(u)\rangle = W_\tau^\dagger(\tau)|\Psi^1(u)\rangle$.

Next, we notice that, since the ACF is the same in both the cases, the corresponding LCs obtained from the moments of the ACF are actually the same (this statement will also be verified later). Therefore, considering the action of the operator O on the Krylov basis $|\tilde{K}_n^1\rangle$, as in Eq. (11), we obtain the following equality:

$$W_\tau^\dagger|\tilde{K}_{n+1}^1\rangle = \frac{1}{\tilde{b}_{n+1}}[(O_{\text{ef}} - \tilde{a}_n)W_\tau^\dagger|\tilde{K}_n^1\rangle - \tilde{b}_n W_\tau^\dagger|\tilde{K}_{n-1}^1\rangle]. \quad (\text{A3})$$

Now comparing this with the action of the operator O_{ef} on $|\tilde{K}_n^2\rangle$, we see that, as expected, two sets of Krylov basis are related by the transformation $|\tilde{K}_n^2\rangle = W_\tau^\dagger(\tau)|\tilde{K}_n^1\rangle$. Using this relation and the expansion of the evolved states in the Krylov basis in Eq. (A2), it is easy to see that the expansion coefficients are actually the same in both cases: $\tilde{\phi}_n^1(u) = \tilde{\phi}_n^2(u)$, so that the corresponding SC, defined as the weighted sum of their modulus squared, are also equal. This proves the equivalence in terms of the SC of the two interpretations of OTOC used in the main text. Furthermore, the fact that the LCs are actually equal in two cases can be verified from the definition of \tilde{a}_n s [in Eq. (12)] and \tilde{b}_n 's (which are just the normalization constants associated with Krylov basis) and noting that, as established above for two operators related by $O_{\text{ef}} = W_\tau^\dagger O W_\tau$, the corresponding Krylov basis vectors are related by $|\tilde{K}_n^2\rangle = W_\tau^\dagger(\tau)|\tilde{K}_n^1\rangle$.

¹⁴For convenience, we suppressed the dependence of different quantities on τ in the following. They can be brought back appropriately from the contexts of cases one considers.

- [1] A. Polkovnikov, K. Sengupta, A. Silva, and M. Vengalattore, *Rev. Mod. Phys.* **83**, 863 (2011).
- [2] I. Bloch, J. Dalibard, and W. Zwerger, *Rev. Mod. Phys.* **80**, 885 (2008).
- [3] J. Kurchan, [arXiv:cond-mat/0007360](#).
- [4] H. Tasaki, [arXiv:cond-mat/0009244](#).
- [5] S. Mukamel, *Phys. Rev. Lett.* **90**, 170604 (2003).
- [6] P. Talkner, E. Lutz, and P. Hänggi, *Phys. Rev. E* **75**, 050102(R) (2007).
- [7] A. Silva, *Phys. Rev. Lett.* **101**, 120603 (2008).
- [8] M. Campisi and J. Gould, *Phys. Rev. E* **95**, 062127 (2017).
- [9] A. Larkin and Yu. N. Ovchinnikov, *Zh. Eksp. Teor. Fiz.* **55**, 2262 (1969) [*Sov. Phys.-JETP* **28**, 1200 (1969)].
- [10] J. Maldacena, S. H. Shenker, and D. Stanford, *J. High Energy Phys.* **08** (2016) 106.
- [11] A. Chenu, I. L. Egusquiza, J. Molina-Vilaplana, and A. del Campo, *Sci. Rep.* **8**, 12634 (2018).
- [12] A. Peres, *Phys. Rev. A* **30**, 1610 (1984).
- [13] R. A. Jalabert and H. M. Pastawski, *Phys. Rev. Lett.* **86**, 2490 (2001).
- [14] A. Goussev, R. A. Jalabert, H. M. Pastawski, and D. Wisniacki, *Scholarpedia* **7**, 11687 (2012).
- [15] T. Gorin, T. Prosen, T. H. Seligman, and M. Znidaric, *Phys. Rep.* **435**, 33 (2006).
- [16] D. E. Parker, X. Cao, A. Avdoshkin, T. Scaffidi, and E. Altman, *Phys. Rev. X* **9**, 041017 (2019).
- [17] J. L. F. Barbón, E. Rabinovici, R. Shir, and R. Sinha, *J. High Energy Phys.* **10** (2019) 264.
- [18] B. Bhattacharjee, X. Cao, P. Nandy, and T. Pathak, *J. High Energy Phys.* **05** (2022) 174.
- [19] A. Dymarsky and A. Gorsky, *Phys. Rev. B* **102**, 085137 (2020).
- [20] A. Dymarsky and M. Smolkin, *Phys. Rev. D* **104**, L081702 (2021).
- [21] A. Kundu, V. Malvimat, and R. Sinha, *J. High Energy Phys.* **09** (2023) 011.
- [22] A. Bhattacharya, P. Nandy, P. P. Nath, and H. Sahu, *J. High Energy Phys.* **12** (2022) 081.
- [23] B. Bhattacharjee, X. Cao, P. Nandy, and T. Pathak, *J. High Energy Phys.* **03** (2023) 054.
- [24] A. Bhattacharya, P. Nandy, P. P. Nath, and H. Sahu, *J. High Energy Phys.* **12** (2023) 066.
- [25] A. Bhattacharyya, D. Ghosh, and P. Nandi, *J. High Energy Phys.* **12** (2023) 112.
- [26] J. Kim, J. Murugan, J. Olle, and D. Rosa, *Phys. Rev. A* **105**, L010201 (2022).
- [27] K. Hashimoto, K. Murata, N. Tanahashi, and R. Watanabe, *J. High Energy Phys.* **11** (2023) 040.
- [28] H. A. Camargo, V. Jahnke, H. S. Jeong, K. Y. Kim, and M. Nishida, [arXiv:2306.11632](#).
- [29] H. A. Camargo, V. Jahnke, K. Y. Kim, and M. Nishida, *J. High Energy Phys.* **05** (2023) 226.
- [30] A. Avdoshkin, A. Dymarsky, and M. Smolkin, [arXiv:2212.14429](#).
- [31] P. Caputa and S. Datta, *J. High Energy Phys.* **12** (2021) 188; **09** (2022) 113.
- [32] D. Patramanis, *PTEP* **2022**, 063A01 (2022).
- [33] E. Rabinovici, A. Sánchez-Garrido, R. Shir, and J. Sonner, *J. High Energy Phys.* **03** (2022) 211.
- [34] M. Alishahiha and S. Banerjee, *SciPost Phys.* **15**, 080 (2023).
- [35] K. Adhikari, S. Choudhury, and A. Roy, *Nucl. Phys. B* **993**, 116263 (2023).
- [36] W. Mück and Y. Yang, *Nucl. Phys. B* **984**, 115948 (2022).
- [37] E. Rabinovici, A. Sánchez-Garrido, R. Shir, and J. Sonner, *J. High Energy Phys.* **07** (2022) 151.
- [38] B. Bhattacharjee, S. Sur, and P. Nandy, *Phys. Rev. B* **106**, 205150 (2022).
- [39] A. Chattopadhyay, A. Mitra, and H. J. R. van Zyl, *Phys. Rev. D* **108**, 025013 (2023).
- [40] B. Bhattacharjee, [arXiv:2302.07228](#).
- [41] B. Bhattacharjee, P. Nandy, and T. Pathak, *J. High Energy Phys.* **08** (2023) 099.
- [42] K. Takahashi and A. del Campo, *Phys. Rev. X* **14**, 011032 (2024).
- [43] D. Patramanis and W. Sybesma, [arXiv:2306.03133](#).
- [44] M. J. Vasli, K. Babaei Velni, M. R. Mohammadi Mozaffar, A. Mollabashi, and M. Alishahiha, [arXiv:2307.08307](#).
- [45] A. A. Nizami and A. W. Shrestha, *Phys. Rev. E* **108**, 054222 (2023).
- [46] K. Adhikari and S. Choudhury, *Fortschr. Phys.* **70**, 2200126 (2022).
- [47] N. Iizuka and M. Nishida, *J. High Energy Phys.* **11** (2023) 096.
- [48] P. Suchsland, R. Moessner, and P. W. Claeys, [arXiv:2308.03851](#).
- [49] A. Bhattacharyya, S. S. Haque, G. Jafari, J. Murugan, and D. Rapotu, *J. High Energy Phys.* **10** (2023) 157.
- [50] Z. Y. Fan, [arXiv:2306.16118](#).
- [51] V. Balasubramanian, P. Caputa, J. M. Magan, and Q. Wu, *Phys. Rev. D* **106**, 046007 (2022).
- [52] V. S. Viswanath and G. Muller, *The Recursion Method Application to Many-Body Dynamics* (Springer, Berlin, 1994).
- [53] C. Lanczos, *J. Res. Natl. Bur. Stand.* **45**, 255 (1950).
- [54] P. Caputa and S. Liu, *Phys. Rev. B* **106**, 195125 (2022).
- [55] P. Caputa, N. Gupta, S. S. Haque, S. Liu, J. Murugan, and H. J. R. Van Zyl, *J. High Energy Phys.* **01** (2023) 120.
- [56] M. Afrasiar, J. K. Basak, B. Dey, K. Pal, and K. Pal, *J. Stat. Mech.* (2023) 103101.
- [57] K. Pal, K. Pal, A. Gill, and T. Sarkar, *Phys. Rev. B* **108**, 104311 (2023).
- [58] M. Gautam, N. Jaiswal, and A. Gill, *Eur. Phys. J. B* **97**, 3 (2024).
- [59] S. Nandy, B. Mukherjee, A. Bhattacharyya, and A. Banerjee, *J. Phys.: Condens. Matter* **36**, 155601 (2024).
- [60] J. Erdmenger, S. K. Jian, and Z. Y. Xian, *J. High Energy Phys.* **08** (2023) 176.
- [61] G. F. Scialchi, A. J. Roncaglia, and D. A. Wisniacki, [arXiv:2309.13427](#).
- [62] M. Gautam, K. Pal, K. Pal, A. Gill, N. Jaiswal, and T. Sarkar, *Phys. Rev. B* **109**, 014312 (2024).
- [63] F. Iglói and H. Rieger, *Phys. Rev. Lett.* **85**, 3233 (2000).
- [64] P. Calabrese and J. Cardy, *Phys. Rev. Lett.* **96**, 136801 (2006).
- [65] P. Calabrese and J. Cardy, *J. Stat. Mech.* (2007) P10004.
- [66] D. W. F. Alves and G. Camilo, *J. High Energy Phys.* **06** (2018) 029.
- [67] H. A. Camargo, P. Caputa, D. Das, M. P. Heller, and R. Jefferson, *Phys. Rev. Lett.* **122**, 081601 (2019).
- [68] A. Polkovnikov and A. Polkovnikov, *Ann. Phys.* **326**, 486 (2011).

- [69] A. Polkovnikov, *Phys. Rev. Lett.* **101**, 220402 (2008).
- [70] A. Chenu, J. Molina-Vilaplana, and A. del Campo, *Quantum* **3**, 127 (2019).
- [71] M. A. Nielsen, [arXiv:quant-ph/0502070](#).
- [72] M. A. Nielsen, M. R. Dowling, M. Gu, and A. M. Doherty, *Science* **311**, 1133 (2006).
- [73] M. A. Nielsen and M. R. Dowling, [arXiv:quant-ph/0701004](#).
- [74] R. Jefferson and R. C. Myers, *J. High Energy Phys.* **10** (2017) 107.
- [75] S. Chapman, M. P. Heller, H. Marrochio, and F. Pastawski, *Phys. Rev. Lett.* **120**, 121602 (2018).
- [76] P. Bueno, J. M. Magan, and C. S. Shahbazi, *J. High Energy Phys.* **09** (2021) 200.
- [77] P. Kumar, S. Mahapatra, P. Phukon, and T. Sarkar, *Phys. Rev. E* **86**, 051117 (2012).
- [78] P. Kumar and T. Sarkar, *Phys. Rev. E* **90**, 042145 (2014).
- [79] N. Jaiswal, M. Gautam, and T. Sarkar, *Phys. Rev. E* **104**, 024127 (2021).
- [80] N. Jaiswal, M. Gautam, and T. Sarkar, *J. Stat. Mech.* (2022) 073105.
- [81] K. Pal, K. Pal, and T. Sarkar, *Phys. Rev. E* **107**, 044130 (2023).
- [82] J. M. Magan, *J. High Energy Phys.* **09** (2018) 043.
- [83] M. Gärttner, J. G. Bohnet, A. Safavi-Naini, M. L. Wall, J. J. Bollinger, and A. M. Rey, *Nat. Phys.* **13**, 781 (2017).
- [84] R. J. Lewis-Swan, A. Safavi-Naini, J. J. Bollinger *et al.*, *Nat. Commun.* **10**, 1581 (2019).
- [85] G. Toth and I. Apellaniz, *J. Phys. A: Math. Theor.* **47**, 424006 (2014).
- [86] L. Pezze and A. Smerzi, *Phys. Rev. Lett.* **102**, 100401 (2009).
- [87] P. Caputa, J. M. Magan, and D. Patramanis, *Phys. Rev. Res.* **4**, 013041 (2022).
- [88] A. Perelomov, *Generalized Coherent States and their Applications* (Springer, New York, 1986).
- [89] M. Ban, *J. Opt. Soc. Am. B* **10**, 1347 (1993).
- [90] C. C. Gerry, *J. Opt. Soc. Am. B* **8**, 685 (1991).
- [91] F. M. Izrailev, *Phys. Rep.* **196**, 299 (1990).
- [92] M. C. Bañuls, J. I. Cirac, and M. B. Hastings, *Phys. Rev. Lett.* **106**, 050405 (2011).
- [93] N. Anand, G. Styliaris, M. Kumari, and P. Zanardi, *Phys. Rev. Res.* **3**, 023214 (2021).
- [94] S. E. Aguilar-Gutierrez and A. Rolph, [arXiv:2311.04093](#).
- [95] T. B. Batalhão, A. M. Souza, L. Mazzola, R. Auccaise, R. S. Sarthour, I. S. Oliveira, J. Goold, G. De Chiara, M. Paternostro, and R. M. Serra, *Phys. Rev. Lett.* **113**, 140601 (2014).
- [96] S. An, J.-N. Zhang, M. Um, D. Lv, Y. Lu, J. Zhang, Z.-Q. Yin, H. Quan, and K. Kim, *Nat. Phys.* **11**, 193 (2015).
- [97] F. Cerisola, Y. Margalit, S. Machluf, A. J. Roncaglia, J. Pablo Paz, and R. Folman, *Nat. Commun.* **8**, 1241 (2017).